Supporting Information

Unraveling the Stress Effects on Optical Properties of Stretchable Rod-Coil Polyfluorene-Poly(*n*-butyl acrylate) Block Copolymer Thin Films

Hui-Ching Hsieh,[a] Chih-Chien Hung,[b] Kodai Watanabe,[c] Jung-Yao Chen,[a]

Yu-Cheng Chiu,[d] Takuya Isono,[c] Yun-Chi Chiang,[a] Renji R. Reghu,[a]

Toshifumi Satoh *[,c] and Wen-Chang Chen *[a,b,e]

[a] Department of Chemical Engineering, National Taiwan University, Taipei 10617, Taiwan.

[b] Institute of Polymer Science and Engineering, National Taiwan University, Taipei 10617, Taiwan.

[c] Graduate School of Chemical Science and Engineering, and Division of Applied Chemistry, Faculty of Engineering, Hokkaido University, Sapporo 060-8628, Japan.

[d] Department of Chemical Engineering, National Taiwan University of Science and Technology, Taipei 10607, Taiwan.

[e] Advanced Research Center for Green Materials Science and Technology, National Taiwan University, Taipei 10617, Taiwan

Table S1. The crack-onset strains of PF_{4k} homopolymer and PF-*b*-PBA copolymers in as-cast and annealed states.

Sample	Crack-onset Strain	
	As-cast Film	**Solvent-annealed Film**
PF_{4k}	0%	0%
PF_{4k}-*b*-PBA_{3k}	50%	25%
PF_{4k}-*b*-PBA_{7k}	100%	75%
PF_{4k}-*b*-PBA_{11k}	-	-

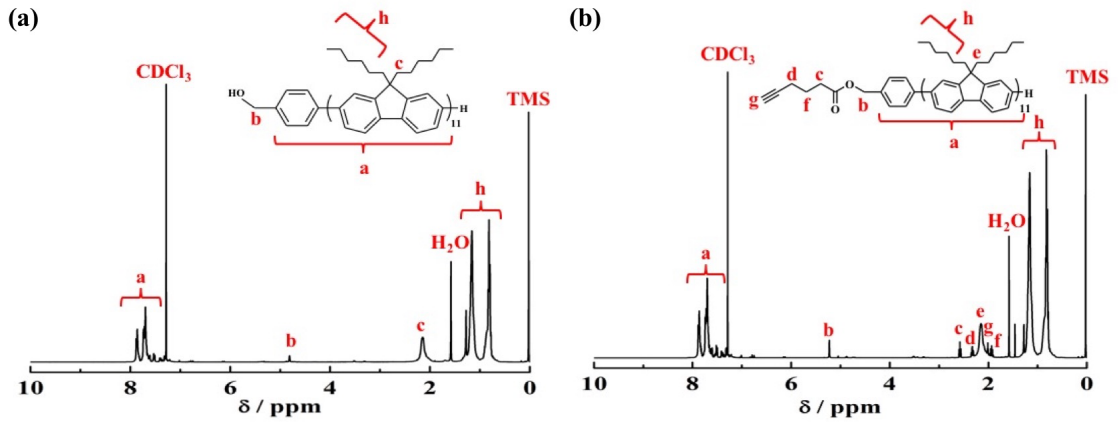

Figure S1. ^{1}H-NMR spectra of (a) PF_{4k}−BnOH and (b) PF_{4k}−C≡CH in $CDCl_3$.

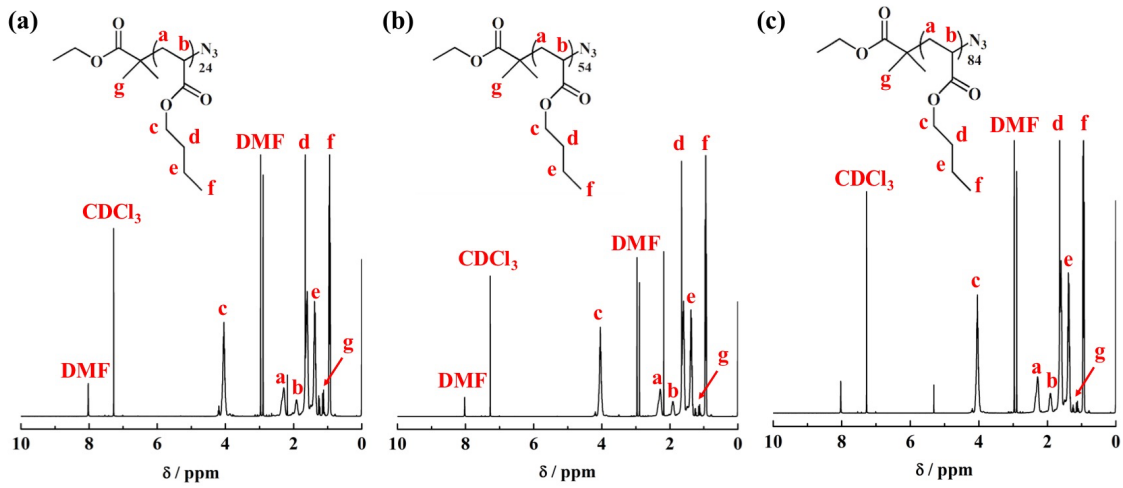

Figure S2. ^{1}H-NMR spectra of (a) PBA_{3k}−N_3, (b) PBA_{7k}−N_3, and (c) PBA_{11k}−N_3 in $CDCl_3$.

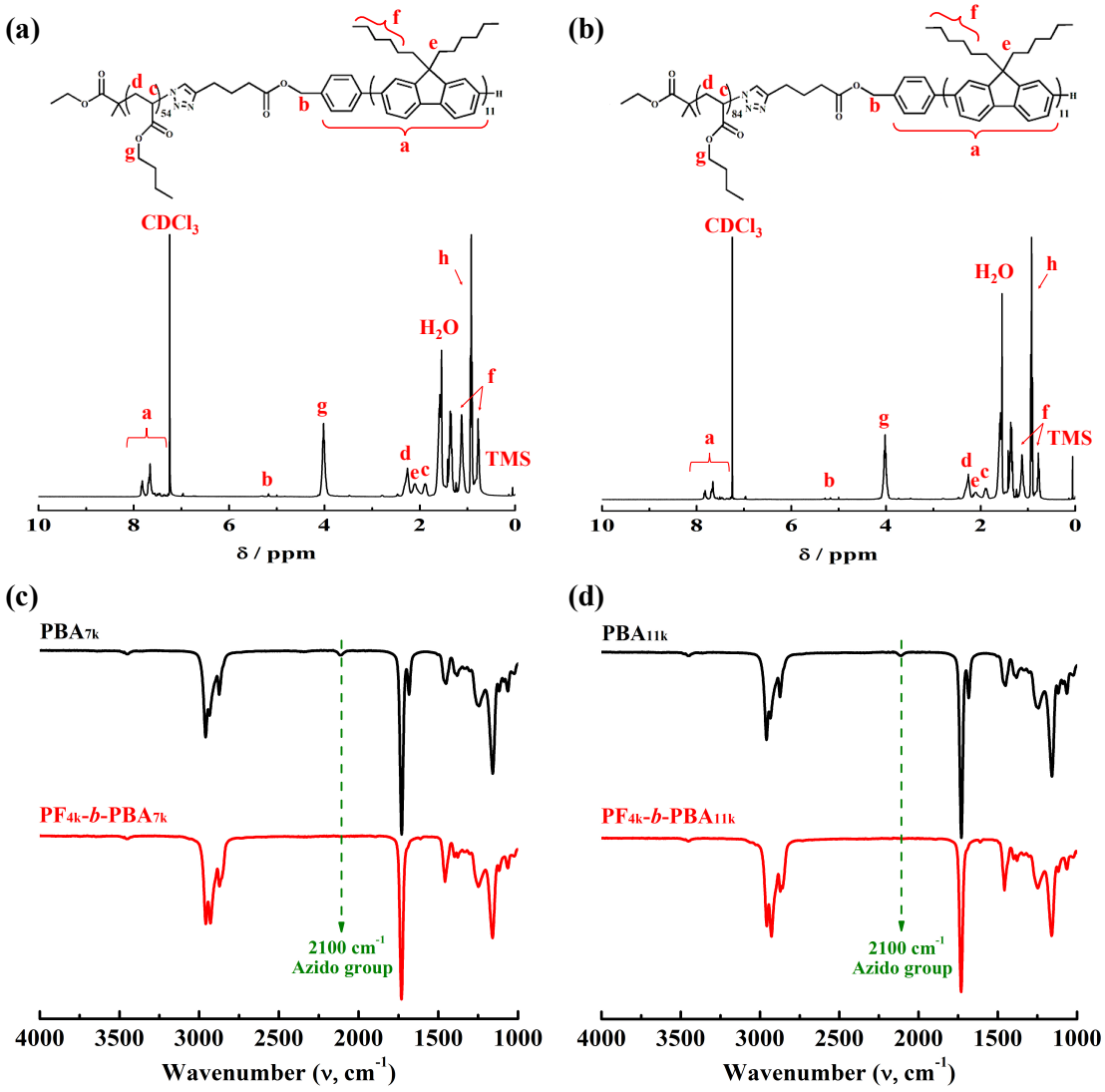

Figure S3. ^{1}H-NMR spectra of (a) PF_{4k}-*b*-PBA_{7k} and (b) PF_{4k}-*b*-PBA_{11k} in $CDCl_3$. FTIR spectra of (c) PBA_{7k}−N_3 and PF_{4k}-*b*-PBA_{7k}; (d) PBA_{11k}−N_3 and PF_{4k}-*b*-PBA_{11k}.

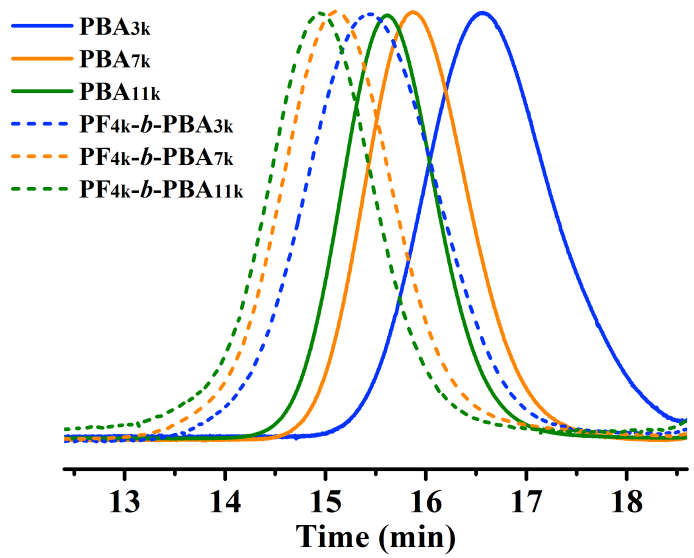

Figure S4. SEC profiles of the PF-*b*-PBA copolymers and their corresponding PBA−N_3 precursors in THF eluent.

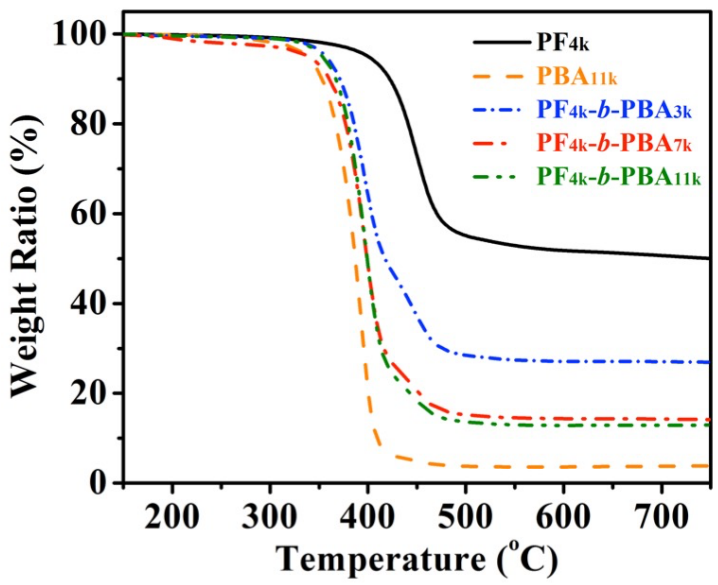

Figure S5. TGA curves of the PF_{4k}, PBA_{11k}−N_3, and PF-*b*-PBA copolymers.

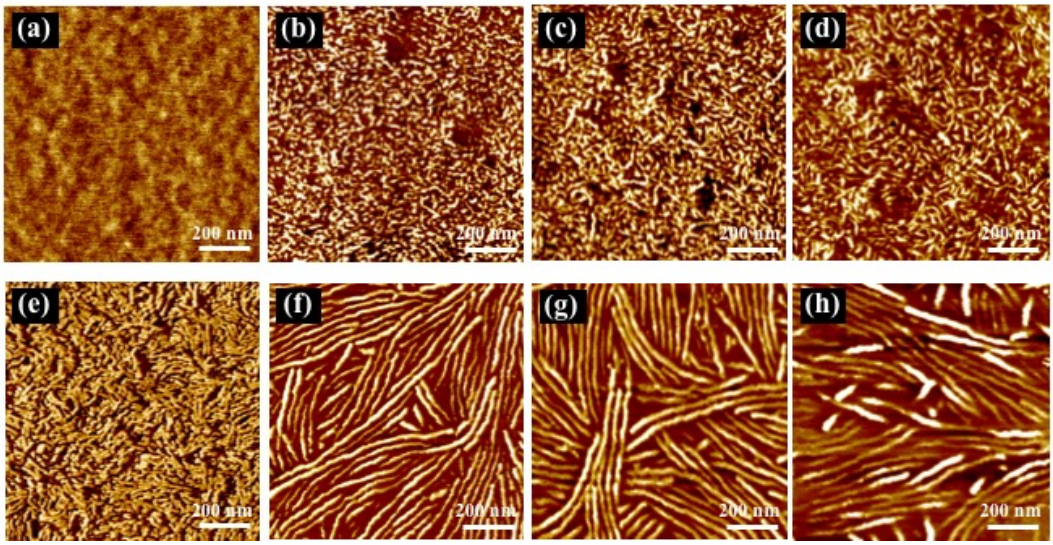

Figure S6. Tapping mode AFM phase images of the (a, e) PF_{4k}, (b, f) PF_{4k}-*b*-PBA_{3k}, (c, g) PF_{4k}-*b*-PBA_{7k}, (d, h) PF_{4k}-*b*-PBA_{11k} as-cast (top row) and solvent-annealed (bottom row) films on bare silicon wafer.

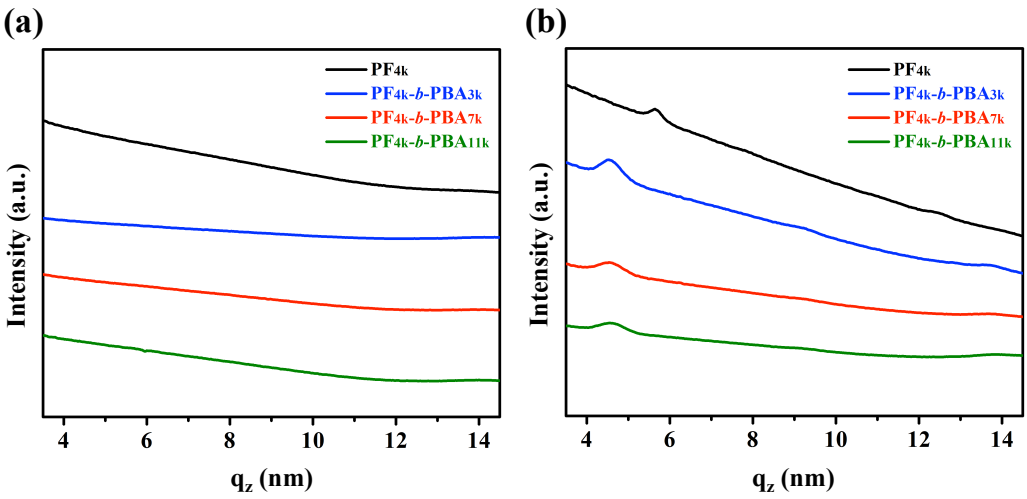

Figure S7. One-dimensional GIXD profiles of the studied polymer thin films in (a) as-cast and (b) solvent-annealed states.

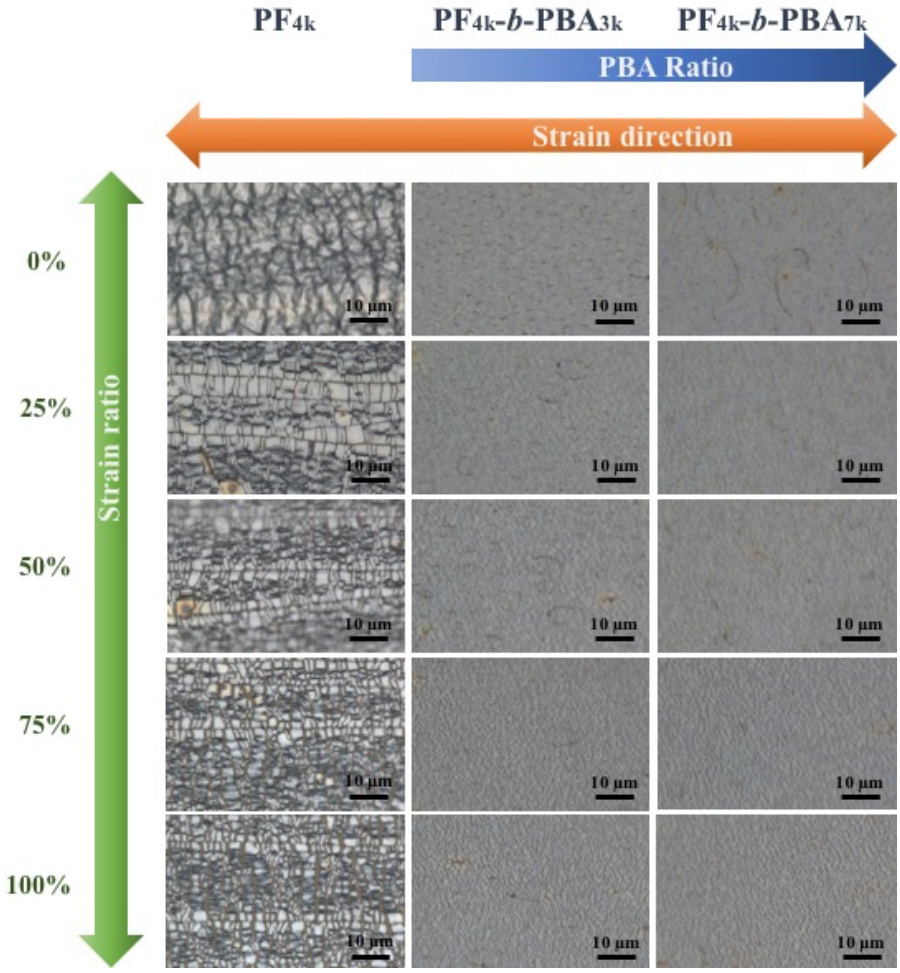

Figure S8. OM images of the annealed studied polymer (i.e., PF_{4k}, PF_{4k}-*b*-PBA_{3k}, and PF_{4k}-*b*-PBA_{7k}) thin films at the strain of 0, 25, 50, 75, and 100%.

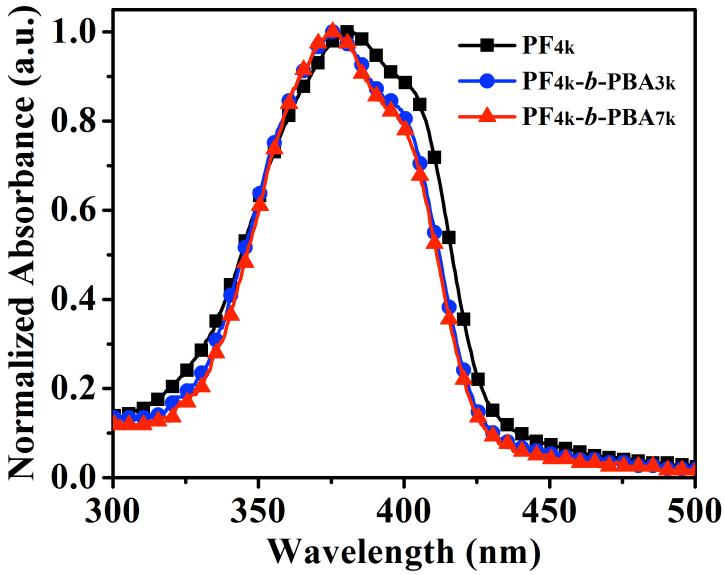

Figure S9. UV-vis absorption spectrum of the annealed PF_{4k}, PF_{4k}-*b*-PBA_{3k}, and PF_{4k}-*b*-PBA_{7k} thin film.

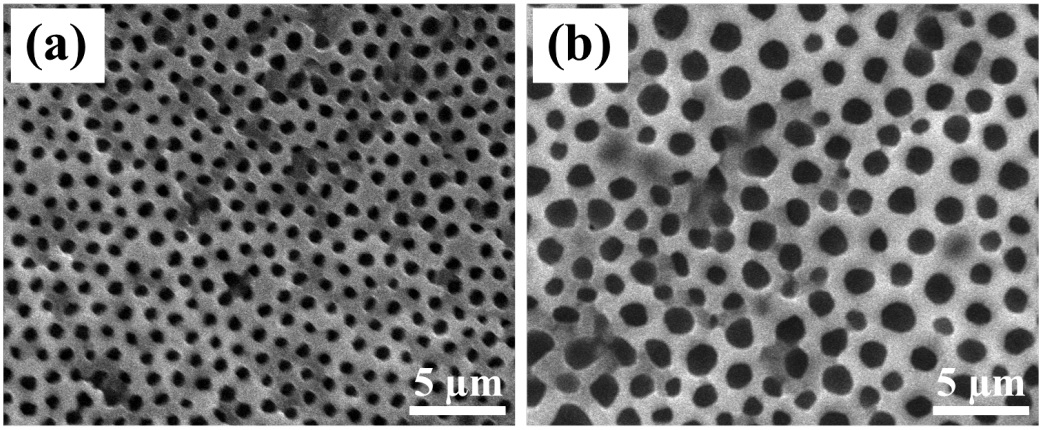

Figure S10. SEM images of the stretchable microporous PF_{4k}-*b*-PBA_{3k} film (a) before and (b) after the stretching/release test at the strain of 20%.